AN ANISOTROPIC TWO-DIMENSIONAL SCATTERING CODE

J.P. Heaton
Boeing Aerospace, P.O. Box 3999, MS 84-01
Seattle, WA 98124-8472

ABSTRACT

A computer code has been developed to predict radar return from two-dimensional cylindrical targets composed of anisotropic, lossy, and inhomogeneous materials. A moment method formulation uses point matching with rectangular domains of pulse basis functions for volumetric elements. Targets may also be composed of thin films including conducting sheets. Particular attention is paid to problems associated with close coupling which involve numerical integration over neighboring domains of basis functions, rectangles which may be very close together as in the case of thin layers of material.

Examples are used to show that analytical integration of singularities associated with close coupling gives results which are superior to the numerical approximations used in typical moment method codes.

The results are of interest for problems involving isotropic as well as anisotropic targets. For example, when a code which calculates close couplings with numerical approximations is applied to a hollow, conducting cylinder, computed radar return may be distorted by introducing conducting elements close to the interior wall of the cylinder. With analytical treatment of singularities, however, there is no distortion. In another example results from codes are compared for the case of a right circular cylinder coated with anisotropic material. Results in good agreement with a series solution taken from the literature are achieved when analytical treatment of singularities is considered. Finally, for the example of a conducting plate it is shown how analytical treatment of singularities makes good results possible for a minimum number of basis functions.

INTRODUCTION

A two-dimensional moment method code ANISO has been writen to predict the radar cross section of targets composed of linear, anisotropic, dielectric and magnetic materials. Special attention is paid to the choice of basis functions and the problem of calculating the couplings between neighboring domains of basis functions, problems which arise in the modeling of typically thin, anisotropic coatings on conducting targets.

To illustrate the problem of choosing basis functions with appropriate domains, consider the thin contour in Figure 1a. This contour is thicker than a thin film but, say, is only one tenth of a wavelength thick. Contours like this, unlike thin films, may support current flow (electric or magnetic) in a direction perpendicular to the contour. Most moment method codes employ the technique developed in [1-2] to approximate such a contour with right circular cylinders (Figure 1b), as a field contribution from a uniform current on a cylinder can be calculated analytically. However, it is desirable to have the option of using rectangular cells which are often more appropriate in approximating layers of materials (Figure 1c). We will see how to accurately calculate field contributions from currents on rectangles.

A case where special attention must be paid to the calculation of couplings between neighboring domains arises when two parallel rectangles each with small thickness compared to width are close together. The coupling involves evaluation of an integral with an integrand which becomes nearly singular as distances between points on the rectangles become close to zero.

Results for a conducting right circular cylinder with an anisotropic coating which is approximated by parallel layers of rectangular cells are shown to be in good agreement with a series solution taken from the

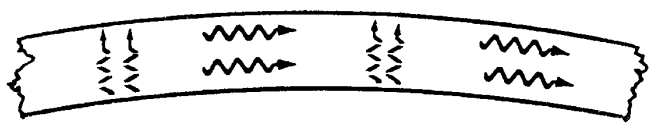

Figure 1a. Thin contour with current flow in tangential and radial directions.

literature. In this example the importance of accurate calculation of coupling between neighboring elements is demonstrated. Another example shows that accurate calculation of couplings is important in isotropic problems such as conducting targets.

ANALYSIS

ANISO is based on two coupled integral equations.

$$\mathbf{E}^{inc}(\mathbf{r}') = \mathbf{E}(\mathbf{r}') + \frac{j}{4}\iint \left\{ \frac{1}{j\omega\epsilon_0}[(\mathbf{J}\cdot\nabla)\nabla + k_0^2\mathbf{J}]F - \mathbf{M}\times\nabla F \right\} ds \tag{1}$$

$$\mathbf{H}^{inc}(\mathbf{r}') = \mathbf{H}(\mathbf{r}') + \frac{j}{4}\iint \left\{ \frac{1}{j\omega\mu_0}[(\mathbf{M}\cdot\nabla)\nabla + k_0^2\mathbf{M}]F + \mathbf{J}\times\nabla F \right\} ds \tag{2}$$

The permittivity and permeability of free space are denoted by ϵ_0 and μ_0, respectively, and ω is the angular frequency. Here $F = H_0^{(2)}(k_0 r)$ is the zero-order Hankel function of the second kind, $k_0 = \omega\sqrt{\epsilon_0\mu_0}$ is the wave number , and $r = |\mathbf{r} - \mathbf{r}'|$ is the distance between a fixed observation point P′ and a variable point P on the target. Also $\mathbf{E}^{inc}$ and $\mathbf{H}^{inc}$ are incident electric and magnetic fields, whereas $\mathbf{E}$ and $\mathbf{H}$ are the total fields. The electric and magnetic current densities $\mathbf{J}$ and $\mathbf{M}$ are related to $\mathbf{E}$ and $\mathbf{H}$ by the following constitutive equations, i.e we have assumed materials to be linear.

$$\mathbf{J} = j\omega\epsilon_0(\overline{\overline{\epsilon}} - 1)\mathbf{E} \tag{3}$$

$$\mathbf{M} = j\omega\mu_0(\overline{\overline{\mu}} - 1)\mathbf{H} \tag{4}$$

In the isotropic case the tensors $\overline{\overline{\epsilon}}$ and $\overline{\overline{\mu}}$ correspond to the familiar complex scalar permittivity ϵ and permeability μ.

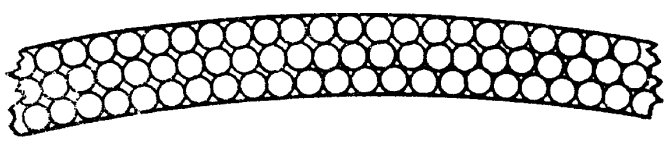

Figure 1b. Thin contour approximated by circular cylinders.

Figure 1c. Thin contour approximated by rectangles.

We may consider the transverse electric (TE) case where the magnetic vectors $\mathbf{H}^{inc}$ and $\mathbf{H}$ are parallel to the long axis of the cylinder in our two-dimensional problem. The transverse magnetic (TM) case follows by interchanging ϵ and μ and considering some sign changes in the calculations. We will consider only rectangular cells as approximating elements. Mutual couplings between rectangles will be analyzed, and the problem of close couplings between rectangles will be discussed in detail. Rectangles of small thickness may be used to model thin films, and in this case the calculated currents in the direction of the thickness will be zero. This result could be anticipated in the analysis, reducing the number of degrees of freedom in the problem. However, this was not done as only basis rectangles with finite thickness have been considered. Current density vectors are assumed to be constant over basis rectangles.

Figure 2 shows how natural coordinate systems are associated with a basis rectangle and a test rectangle. Vectors in the figure are unit vectors. In the TE case terms corresponding to coupling between a basis and test rectangle can be arranged in a matrix TE.

$$\begin{pmatrix} H_z \\ \mathbf{E}\cdot\hat{\mathbf{l}}_n \\ \mathbf{E}\cdot\hat{\mathbf{t}}_n \end{pmatrix} = \begin{pmatrix} TE(1,1) & TE(1,2) & TE(1,3) \\ TE(2,1) & TE(2,2) & TE(2,3) \\ TE(3,1) & TE(3,2) & TE(3,3) \end{pmatrix} \begin{pmatrix} M_z \\ J_l \\ J_t \end{pmatrix} \tag{5}$$

Here H_z is the magnitude of the vector $\mathbf{H}$ which points in the direction of the long axis of the cylinder. Similarly, M_z is the only component of $\mathbf{M}$. Also J_l and J_t are coordinates of $\mathbf{J}$ in the natural coordinte system associated with the basis rectangle. Elements of the 3×3 matrix TE are obtained by substituting pulse basis functions into equations (1) and (2), and the elements in the vector on the left hand side of the equation are field evaluations at the center of the test strip. Coupling terms for all rectangles are arranged in a large system matrix composed of submatrices of the type TE in (5).

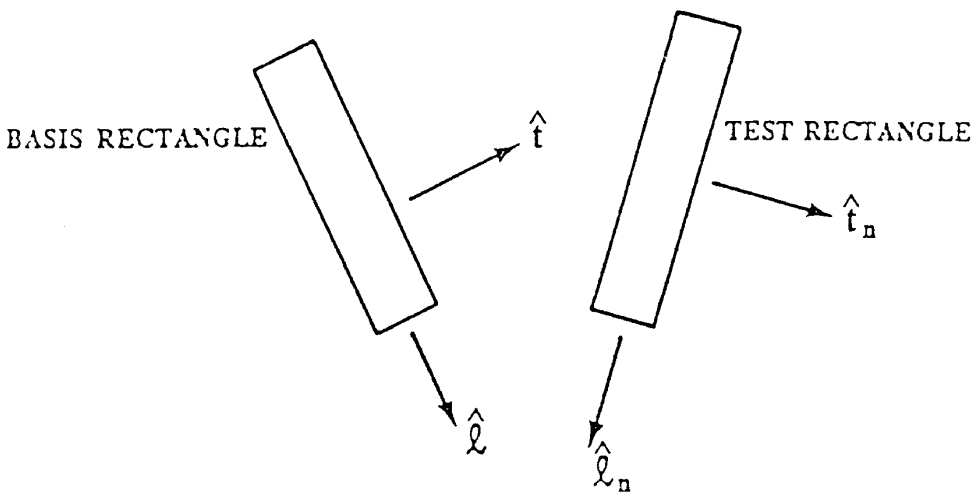

Figure 2. Pair of basis and test rectangles.

We will assume $\overline{\overline{\epsilon}}$ and $\overline{\overline{\mu}}$ can be represented by diagonal matrices in natural coordinate systems associated with basis elements. This is a restriction on $\overline{\overline{\epsilon}}$ and $\overline{\overline{\mu}}$ which, nevertheless, includes an important class of problems.

The following calculations will deal first with self terms, i.e. the case where basis and test rectangles coincide (observation point at the center of the basis rectangle), and then with non-self terms. The off-diagonal elements are all zero in the case of self terms and will be considered first.

Since $\hat{\mathbf{l}} \times \nabla F = \hat{\mathbf{t}} \cdot \nabla F \hat{\mathbf{z}}$, integrating first in the t-direction shows TE(2,1)=0. Similar arguments show the remaining off-diagonal elements are zero.

The difficulty in calculating diagonal terms is that the Hankel function $H_0^{(2)}$ becomes singular at the origin. To integrate $H_0^{(2)}$ we may write

$$\begin{aligned}\iint H_0^{(2)}(k_0\sqrt{l^2+t^2})\,dl\,dt = \\ \iint \{H_0^{(2)}(k_0\sqrt{l^2+t^2}) + \frac{2j}{\pi}\log(k_0\sqrt{l^2+t^2}/2) + 0.5722\}\,dl\,dt \\ - \frac{2j}{\pi}\iint \{\log(k_0\sqrt{l^2+t^2}/2) + 0.5772\}\,dl\,dt\end{aligned} \tag{6}$$

The first integral on the right hand side of (6) can be evaluated numerically. In fact, the value of the integrand is unity at the origin. Due to symmetry of the rectangle, only three Hankel function evaluations are required when a 3 point Simpson's rule is used in each direction. The second integrand on the right hand side is the small argument approximation to the Hankel function and can be evaluated analytically. Here it is necessary to compute the indefinite integral

$$\iint \log(l^2+t^2)\,dl\,dt$$

First use the integration-by-parts substitution

$$\log(l^2+t^2) = u \qquad dv = dl$$

$$\frac{2l}{l^2+t^2}\,dl = du \qquad v = l$$

Then integrate in the t-direction using the parts substitution

$$tan^{-1}(\frac{l}{t}) = u \qquad dv = t\,dt$$

$$\frac{-l}{l^2+t^2}\,dt = du \qquad v = \frac{t^2}{2}$$

The indefinite integral is

$$\iint \log(l^2+t^2)\,dl\,dt = lt\log(l^2+t^2) - 3lt + l^2 tan^{-1}(\frac{t}{l}) + t^2 tan^{-1}(\frac{l}{t}) \tag{7}$$

The desired definite integral for a rectangle of width L and thickness T is

$$\begin{aligned}-\frac{2j}{\pi}\int_{-L/2}^{L/2}\int_{-T/2}^{T/2}[\log(k_0\sqrt{(l^2+t^2)/2} + 0.5772]\,dt\,dl \\ = -\frac{2j}{\pi}[0.5772LT + \{LT\log(k_0\sqrt{(L/2)^2+(T/2)^2}/2) \\ - \frac{3}{2}LT + \frac{L^2}{2}tan^{-1}(\frac{T}{L}) + \frac{T^2}{2}tan^{-1}(\frac{L}{T})\}]\end{aligned} \tag{8}$$

To calculate TE(1,1) use (4) in (2) with a 3 point Simpson's rule applied to the integrand to be evaluated numerically to get

$$\begin{aligned}\mathrm{TE}(1,1) =& \frac{1}{(j\omega\mu_0(\mu_z-1))} + \frac{\omega\epsilon_0}{4}\left\{\frac{TL}{36}(4(H_0(k_0\sqrt{(T/2)^2+(L/2)^2})+\right.\\ &\frac{2j}{\pi}(\log(k_0\sqrt{(T/2)^2+(L/2)^2}/2)+0.5772))+\\ &8(H_0(k_0T/2)+\frac{2j}{\pi}(\log(k_0T/4)+0.5772))+\\ &4(2(H_0k_0L/2)+\frac{2j}{\pi}(\log(k_0L/4)+0.5772))+4))-\\ &\frac{2j}{\pi}(LT(-0.9228+\log(k_0\sqrt{(L/2)^2+(T/2)^2}/2))+\\ &\left.\frac{L^2}{2}tan^{-1}\left(\frac{T}{L}\right)+\frac{T^2}{2}tan^{-1}\left(\frac{L}{T}\right)\right)\Big\}\end{aligned} \tag{9}$$

To calculate TE(2,2) first calculate

$$\hat{\mathbf{l}}\cdot\iint\nabla(\hat{\mathbf{l}}\cdot\nabla F)\,ds = k_0\iint\frac{d^2F}{dl^2}\,dl\,dt = -2k_0\int\cos\theta H_1^{(2)}(k_0\sqrt{(L/2)^2+t^2})\,dt \tag{10}$$

where θ is the angle between a vector parallel to the basis strip and a vector from the center of the strip to a point on the strip. Numerical integration of (10) with a 3 point Simpson's rule in the t-direction gives

$$\hat{\mathbf{l}}\cdot\iint\nabla(\hat{\mathbf{l}}\cdot\nabla F)\,ds = -\frac{k_0TL}{3}\left\{\frac{L}{\sqrt{(L/2)^2+(T/2)^2}}H_1^{(2)}(k_0\sqrt{(L/2)^2+(T/2)^2}+4H_1^{(2)}(k_0L/2))\right\} \tag{11}$$

Next, calculate the integral of the zero-order Hankel function as in TE(1,1). The total result is

$$\begin{aligned}\mathrm{TE}(2,2) =& \frac{1}{(j\omega\epsilon_0(\epsilon_l-1))}+\\ &-\frac{k_0TL}{12\omega\epsilon_0}\left\{\frac{L}{\sqrt{(L/2)^2+(T/2)^2}}H_1^{(2)}(k_0\sqrt{(L/2)^2+(T/2)^2})+4H_1^{(2)}(k_0L/2)\right\}\\ &+\frac{\omega\mu_0T}{24}\left\{\frac{L}{3}(2H_0^{(2)}(k_0\sqrt{(L/2)^2+(T/2)^2})+4H_0^{(2)}(k_0L/2))\right.\\ &+4\left[\frac{L}{6}(2H_0^{(2)}(k_0L/2)+\frac{2j}{\pi}(\log(k_0L/4)+0.5772)+4)\right.\\ &\left.\left.-\frac{2j}{\pi}(L\log(k_0L/4)+0.4228L)\right]\right\}\end{aligned} \tag{12}$$

Here ϵ_l is the permittivity corresponding to the l-direction.

TE(3,3) is similar to TE(2,2) except with L and T interchanged and $\hat{\mathbf{l}}$ replaced bt $\hat{\mathbf{t}}$.

Next, we indicate how to calculate non-self terms. Here the observation point is on the test rectangle which is away from the basis rectangle as depicted in Figure 2.

TE(1,1) is calculated as in the self term. The numerical integration involves several computations of the Hankel function, and the small argument approximation has the indefinite integral (7).

TE(1,2)=$-\frac{j}{4}k_0\hat{z}\cdot\iint H_1^{(2)}(k_0r)\hat{\mathbf{l}}_n\times\hat{\mathbf{r}}\,dl\,dt$ where $\hat{\mathbf{r}}$ is the gradient of r. This integral may be evaluated by considering the small argument expression and integrating the resulting integrand analyically. As in the case

of self terms the remaining contribution can be integrated numerically. The vector $\hat{\mathbf{l}}_n$ may be expressed in terms of the basis vectors $\hat{\mathbf{t}}$ and $\hat{\mathbf{l}}$ in Figure 2. Then the vector product will include two terms , one involving $\cos\theta$ and one involving $\sin\theta$ where θ is the angle between $\hat{\mathbf{r}}$ and $\hat{\mathbf{l}}$. The small argument approximation times the cosine term is

$$\left\{\frac{k_0 r}{2}+\frac{j}{\pi}\frac{2}{k_0 r}\right\}\cos\theta=\frac{k_0(l_0-l)}{2}+\frac{j}{\pi}\frac{2(l_0-l)}{k_0 r^2} \tag{13}$$

Here l_0 is the l-coordinate of the observation point. The indefinite double integral is

$$\begin{aligned}-\frac{k_0(l-l_0)^2 t}{4}+\frac{j}{\pi k_0}\int \log\{(l-l_0)^2+(t-t_0)^2\}\,dt \\ =-\frac{k_0(l-l_0)^2 t}{4}-\frac{j}{\pi k_0}\left[(t-t_0)\log((l-l_0)^2+(t-t_0)^2)-\right. \\ \left.2\left\{(t-t_0)-(l-l_0)\tan^{-1}\left(\frac{t-t_0}{l-l_0}\right)\right\}\right]\end{aligned} \tag{14}$$

The terms TE(1,3), TE(3,1), and TE(2,1) are similar.

For TE(2,2) we have

$$\begin{aligned}TE(2,2)&=\frac{\omega\mu_0}{4}\hat{\mathbf{l}}\cdot\hat{\mathbf{l}}_n\iint H_0(k_0 r)\,dl\,dt-\frac{1}{4}\frac{1}{\omega\epsilon_0}\hat{\mathbf{l}}_n\cdot\iint\nabla(\hat{\mathbf{l}}\cdot\nabla F)\\ &=\frac{\omega\mu_0}{4}\hat{\mathbf{l}}\cdot\hat{\mathbf{l}}_n\iint H_0(k_0 r)\,dl\,dt\\ &\quad+\frac{k_0}{4\omega\epsilon_0}\hat{\mathbf{l}}_n\cdot\int\left\{H_1^{(2)}(k_0\,|\mathbf{r}-\tfrac{1}{2}\mathbf{l}|)\right.\\ &\quad\left.-H_1^{(2)}(k_0\,|\mathbf{r}+\tfrac{1}{2}\mathbf{l}|)\right\}\hat{\rho}\,dt\end{aligned} \tag{15}$$

Here $H_1^{(2)}$ is the first-order Hankel function and $\mathbf{l}=L\hat{\mathbf{l}}$. We have been able to integrate in the l-direction using properties of the gradient. Notice $|\rho-\frac{1}{2}\mathbf{l}|$ is the distance from the observation point to a point sliding along the edge of the test rectangle in the t-direction. This calculation of TE(2,2) differs from a previous approach taken in Boeing codes. For example, in the isotropic code LINKS [3-4] properties of the gradient have not been exploited to integrate in the l-direction, rather a second order difference involving the zero order Hankel function is used. It is this second order difference which creates havoc with close coupling. An example illustrating this point is included at the end of the section on validation.

The first integral in the expression for TE(2,2) can be evaluated as before. The idea of integrating a term involving the small argument of a Hankel function can be applied to the second integral, too. For example, the indefinite integral of the small argument approximation of $H_1^{(2)}(k_0\rho)$ multiplied by $\cos\theta$ is

$$\int\left[\frac{k_0(l-l_0)}{2}+\frac{2j}{\pi k_0}\frac{(l-l_0)}{\rho^2}\right]dt=\frac{k_0(l-l_0)t}{2}-\frac{2j}{\pi k_0}\tan^{-1}\left(\frac{(t-t_0)}{(l-l_0)}\right) \tag{16}$$

Similarly for $H_1^{(2)}(k_0\rho)\sin\theta$ we get

$$\int\left[\frac{k_0(t-t_0)}{2}+\frac{2j}{\pi k_0}\frac{(t-t_0)}{\rho^2}\right]dt=-\frac{k_0(t-t_0)^2}{4}-\frac{j}{\pi k_0}\log[(l-l_0)^2+(t-t_0)^2] \tag{17}$$

The integrand in the second integral in the expression for TE(2,2) is the sum of the Hankel functions multiplied by $\sin\theta$ and $\cos\theta$, each multiplied by a constant.

The remaining terms are similar to TE(2,2), involving the possible combinations obtained by replacing $\hat{\mathbf{l}}$ or $\hat{\mathbf{t}}$ by $\hat{\mathbf{l}}_n$ or $\hat{\mathbf{t}}_n$ where the latter two vectors are associated with the observation strip.

Although the calculations we have discussed are important in the case of close coupling, cheaper calculations should be made when the basis rectangle and test rectangle are not close together. In ANISO a test is performed to see if the coupling involves arguments in Hankel functions which are small enough to warrant refined calculations. A rule of thumb for making this decision follows. If ρ_1 and ρ_2 are the minimum and maximum distances from the obsevation point to grid points on the basis rectangle, and if ρ_0 is the distance between centers of rectangles, crude integration is performed when $k_0\rho_1 \gg 1$ and $|k_0\rho_2 - k_0\rho_1| < 0.1$. In this case the first inequality guarantees the large argument approximation to the Hankel function may be used:

$$H_\nu^{(2)}(k_0\rho) \approx \sqrt{\frac{2}{\pi\rho}}\, exp(-j(k_0\rho\frac{\nu\pi}{2} - \frac{\pi}{4})), \qquad k_0\rho \gg 1, \quad \nu = 0, 1 \tag{18}$$

The second inequality guarantees that $H_\nu^{(2)}(k_0\rho)$ can be considered constant over the strip.

EXAMPLES AND VALIDATION

The following examples test the close coupling equations of ANISO. The first example which is an isotropic case is a configuration of conducting sheets. This example compares the radar cross section of a flat plate with a conducting, hollow, rectangular cylinder and a cylinder containing a conducting sheet. Comparisons of the radar cross section of these targets for both crude and refined evaluations of integrals are broken down into four test cases. Refined integration involves extraction of singularities, whereas crude integration involves only evaluations of the Hankel functions. In all cases surfaces are uniformly subdivided with ten basis rectangles per wavelength.

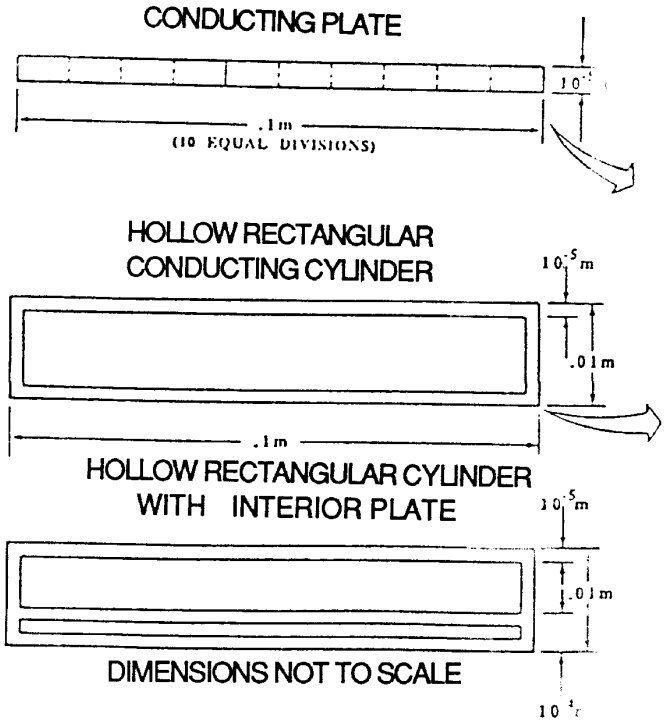

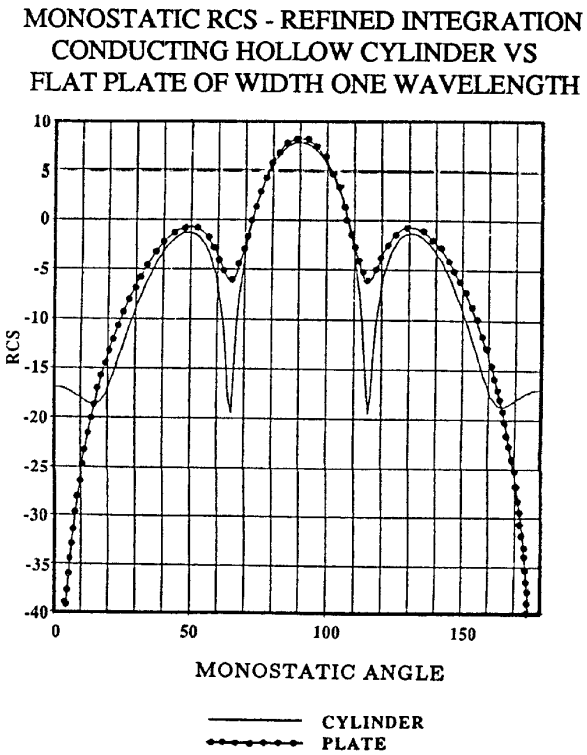

Figure 3. Flat plate versus hollow cylinder.
TE POLARIZATION

Figure 3 shows the flat plate verses the hollow conducting cylinder for refined integration. Figure 4 compares crude and refined integration for the hollow cylinder with an interior conduction sheet close to the cylinder wall. From the standpoint of physics the interior metal should make no contribution to the radar cross section. Indeed, for refined evaluation the plots of the hollow cylinder and the cylinder containing the sheet are virtually coincident.

Figure 5 shows an annular configuration of anisotropic material which has been partitioned into rectangles, the inner surface being a thin conducting contour. The angle in the figure is the bistatic angle. Also $\epsilon_t = 6$ and $\epsilon_l = 1.5$ with $\mu_z = 2$. Also included in Figure 5 is the bistatic return resulting from the crude and refined integration as well as a few points obtained from a code based on a series solution [5]. It is clear that refined integration improves accuracy.

Finally, we will include an example from the LINKS code which illustrates the problem associated with the finite difference calculation of certain matrix elements. (TE(2,2) is the culprit in the following example.) Figure 6a shows the monostatic return for a flat conducting plate eight wavelengths in width. Two uniform subdivisions of ten and twenty-five strips per wavelength are considered. The points per wavelength required to get a good solution is unsatisfactory. In particular, the extreme side lobes are not high enough. Figure 6b shows LINKS with thirty-five strips per wavelength versus ANISO with ten strips per wavelength. ANISO gives a good result for a reasonable number of strips per wavelength whereas LINKS does not.

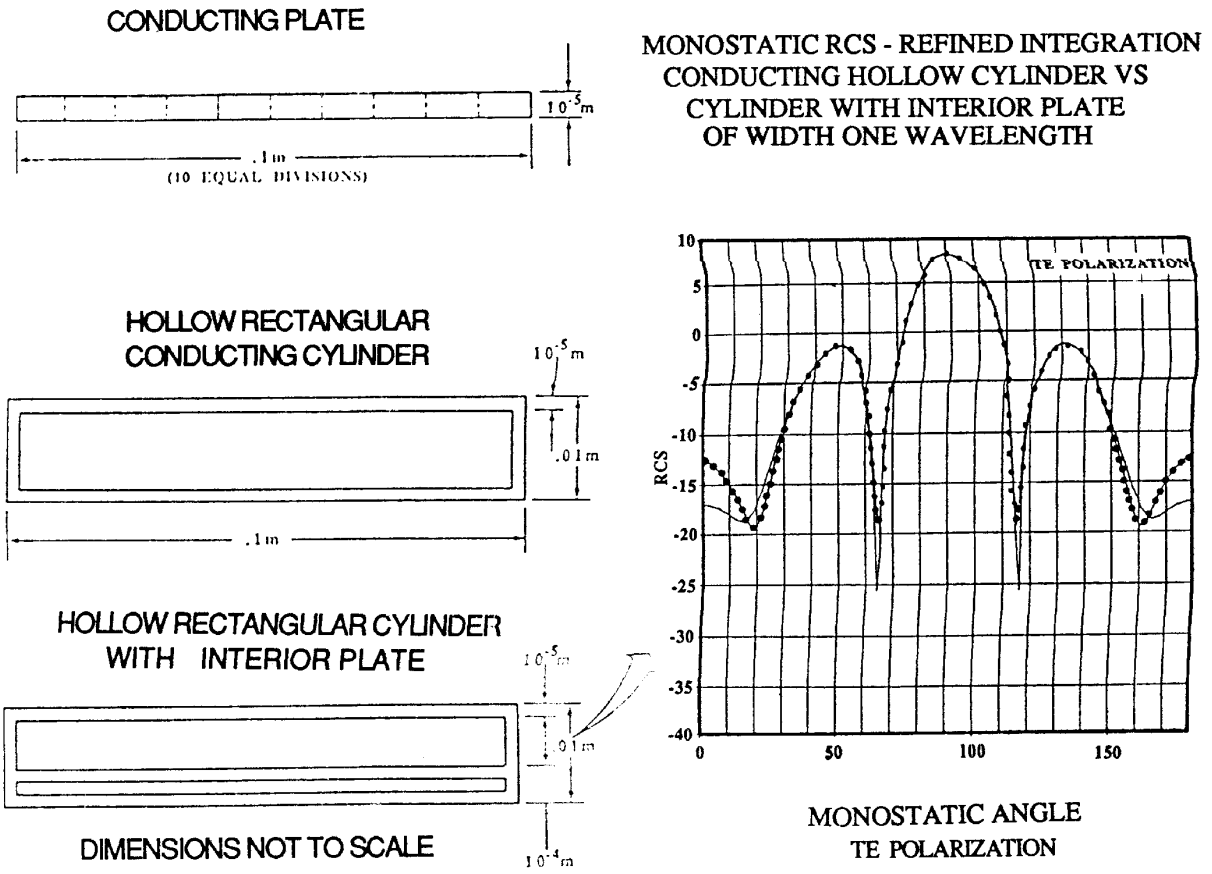

Figure 4. Crude and refined integration for hollow cylinder with conducting sheet.

CONCLUSION

The two-dimensional code ANISO has been validated with isotropic and anisotropic test cases. The importance of accurate computation of close couplings has been demonstrated. Computations of this type, which involve integration of functions near singularities, always arise in moment method codes, isotropic or anisotropic, with either polarization.

Another enhancement to the code might include special treatment of thin films (including conducting sheets) which reduce the number of degrees of freedom in the problem by introducing basis strips which do not allow for current flow in the normal direction. A further enhancement might provide for basis functions with triangular domains, since triangles may be used to approximate two-dimensional regions.

REFERENCES

[1] Richmond, J. H., "Scattering by a dielectric cylinder of arbitrary cross section shape," IEEE *Trans. on Antennas and Propagation*, May 1965.

[2] Richmond, J. H., "TE-wave scattering by a dielectric cylinder of qarbitrary cross-section shape," IEEE *Trans. on Antennas and Propagation*, July, 1966.

[3] Lin, J. L., "Electromagnetic scattering from two-dimensional lossy dielectric bodies - for H-polarized wave illumination," Boeing document 2-3745-RHW-039, November 1982.

[4] Damaskos, N. J., "VERSION V - An integral equation - based computer design program for E-polarization scattering by resistive, dielectric, metallic 2-dimensional bodies," N. J. Damaskos, Inc., Concordville, Pa., November, 1981.

[5] H. Massoudi, N.J. Damaskos, P.L.E. Uslenghi, "Scattering by a composite and anisotropic circular cylindrical structure: exact solution," Electromagnetics 8:71-83, 1988.

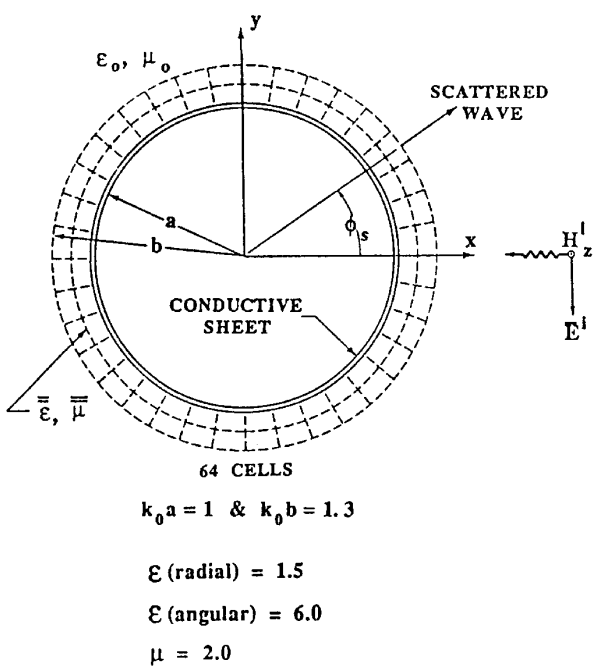

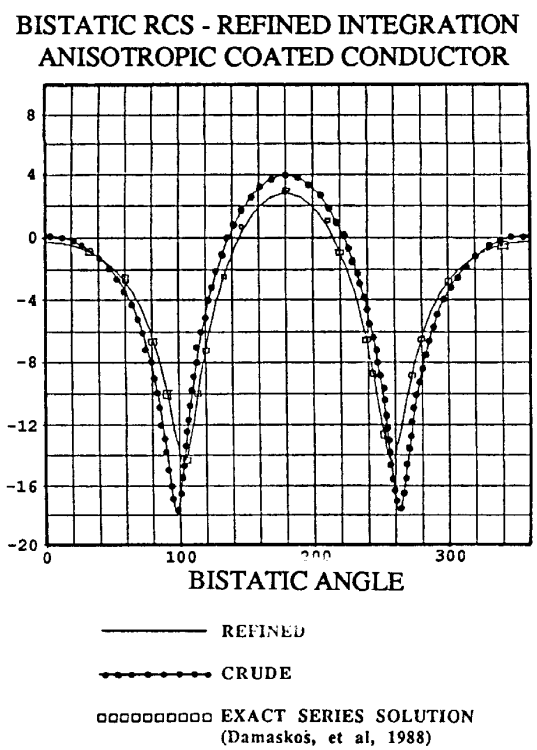

Figure 5. Conducting cylinder with anisotropic coating

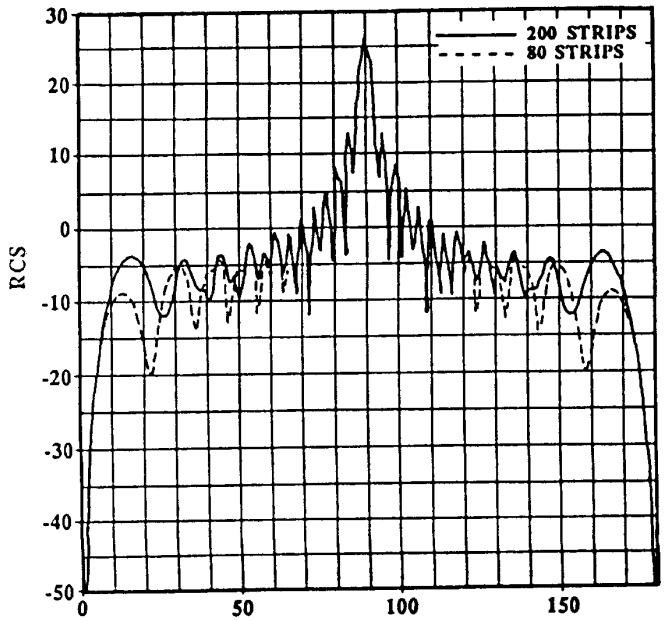

Figure 6a. LINKS result for flat plate.

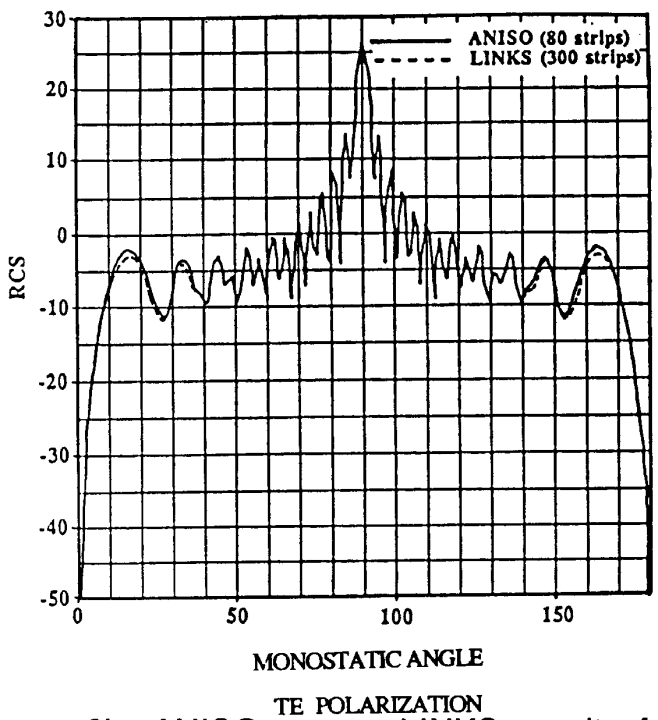

Figure 6b. ANISO versus LINKS results for flat plate.